good agreement with the theoretical value of 2.78 moles.

According to equation 4, two moles of hydroxamic acid should be consumed per mole of Sarin. The competing side reaction between aqueous solvent and Sarin will reduce this value by an amount which will depend on both pH and concentration of hydroxamic acid. Under the conditions of this study the side reaction between Sarin and solvent occurs to only a minor extent. On the other hand, the side reaction between phenyl isocyanate and aqueous solvent (competitive with reaction 3) is appreciable. In the absence of Sarin, the reaction of phenyl isocyanate (18.5 μmoles) with an excess of benzohydroxamic acid (163 μmoles) in 275 ml. of 0.1 M potassium nitrate at 7.6 consumed only 13.2 $\pm$ 0.2 μmole of hydroxamic acid, 0.72 mole of hydroxamic acid per mole of phenyl isocyanate. Hence, according to the postulated reaction series, the reaction of Sarin and benzohydroxamic acid under the same conditions, should consume 1.72 moles of hydroxamic acid per mole of Sarin, which is in close agreement with the observed value of 1.67 moles.

It was considered highly unlikely that reaction 3, the step which involves the very reactive phenyl isocyanate molecule would contribute to the kinetic picture. Under the conditions of this study, phenyl isocyanate was observed to react with water or benzohydroxamic acid at an immeasurably rapid rate.[34] Also, the rate of acid production from the aqueous hydrolysis of benzohydroxamic acid under our reaction conditions is zero order (Fig. 3B), and the pseudo-first-order side reaction

(34) At pH 7.6, a half-time of 25 sec. was observed with the Autotitrator when 10 δ of phenyl isocyanate in 10 ml. of acetone was added to 300 ml. of 0.1 N KNO$_4$ solution. However, this represents the limiting rate of operation of the Autotitrator rather than the actual rate of reaction.

between Sarin and aqueous solvent is so small in magnitude that it can be safely ignored.

Thus the experimental data clearly support the postulated reaction series and indicate that step 1, the phosphonylation reaction, is rate determining. Hence, it is established that the rate of production of acid can be employed satisfactorily for comparison of the relative reactivity of Sarin with a series of hydroxamic acids.[35]

It is interesting to note that the rate of reaction of Sarin with benzohydroxamate ion is very large as compared with the rate observed in reaction with anions of other weak acids. This suggests the operation of powerful stereoelectronic effects in the former reaction and is perhaps analogous in process to that proposed for the rapid reaction of catechol (as compared to phenol) with DFP[36] (cf. structures A and B) and Sarin.[37]
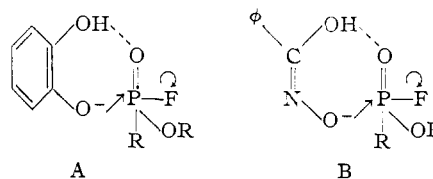
A   B

(35) Barring an inversion in the relative rates of steps 1 and 2, which would be evidenced by a change in the over-all kinetic picture.

(36) B. J. Jandorf, T. Wagner-Jauregg, J. J. O'Neill and M. A. Stolberg, THIS JOURNAL, **73**, 5202 (1951).

(37) J. Epstein, D. H. Rosenblatt and M. M. Demek, ibid., **78**, 341 (1956).

ARMY CHEMICAL CENTER, MD.

Effects of Hydrostatic Pressure upon Sedimentation in the Ultracentrifuge

BY HIROSHI FUJITA[1]

Effects of hydrostatic pressure upon the sedimentation process in the ultracentrifuge are investigated mathematically on the basis of the Lamm sedimentation equation without the diffusion term. In accordance with a recent article by Oth and Desreux, the sedimentation coefficient, s, is assumed to vary linearly with pressure. First the case in which s is dependent only on pressure is considered in detail, and the concentration gradient curve for an illustrative case is computed using the analytical solution obtained, in order to show the characteristic feature of pressure-dependent sedimentation. Methods for correcting measured sedimentation coefficient values to those at a pressure of one atmosphere are shown. Consideration is then extended to the case of s dependent both on pressure and concentration. Because of the complexity of the general solution obtained, its numerical calculation is not attempted. On the basis of these results Oth and Desreux's treatment of a similar problem is criticized.

At speeds of rotation usually employed in velocity sedimentation measurements, a large pressure difference, which may amount to several hundred atmospheres, is produced between the meniscus and the bottom of the cell. Since the viscosity and density of the solvent and the specific volume of the solute may vary with pressure, it is expected that sedimentation processes in such a field of high pressure gradient should differ more or less from those in a field of uniform pressure. In order to attain a high precision in the evaluation of the molecular weight of a given substance by means of sedimentation measurements, a correction must be made to sedimentation data with respect to this pressure effect, along with, among other things, the elimination of the concentration effect by means of extrapolation to infinite dilution.

This problem was first considered by Mosimann

(1) On leave from the Department of Fisheries, Faculty of Agriculture, Kyoto University, Maizuru, Japan.

and Signer[2] and was recently worked out more specifically by Oth and Desreux[3] and by Cheng and Schachman.[4] Singer[5] has discussed the effect of pressure upon the configuration of sedimenting flexible macromolecules using Kuhn's model of coiled long chain molecules. The purpose of the present paper is to consider a similar problem as dealt with by Oth and Desreux on the basis of the differential equation for sedimentation presented by Lamm.[6] It will be essentially a mathematical refinement and extension of the results which they derived on the basis of empirical considerations.

Basic Equations

It has been shown in a recent paper[7] that, even when there is a concentration dependence of the sedimentation coefficient, the rate of movement of the maximum of a concentration gradient curve can be represented fairly closely by means of the solution to the Lamm sedimentation equation without the diffusion term, if the reduced time τ and the parameter ϵ defined in reference 7 are sufficiently small compared with unity. In the present paper, it is presumed that this is also the case for pressure-dependent sedimentation if the above-mentioned assumptions are satisfied. Thus the differential equation is adopted as the basis of this

$$\frac{\partial C}{\partial t} = -\frac{\partial}{r \partial r}(r^2 \omega^2 s C) \qquad (1)$$

mathematical analysis. In equation 1, C is the concentration of the solute (which is assumed to be single and homogeneous), t is the time, r is the radial distance measured from the center of rotation, ω is the angular speed of rotation, and s is the sedimentation coefficient. Equation 1 can be derived from the complete Lamm sedimentation equation (see, for example, equation 1 in reference 7) by setting the diffusion coefficient D equal to zero. Cheng and Schachman[4] have treated cases in which the solvent has a density almost equal to that of the sedimenting particles, in order that a sufficiently large effect of pressure may be observed experimentally. It should be noted, however, that equation 1 is no longer effective for such cases, because sedimentation coefficients measured in such systems are likely to be so small that the assumption $\epsilon \ll 1$, on which the validity of equation 1 is based, no longer holds. In other words, in such systems the effect of diffusion should be appreciable, and we have to resort to the complete Lamm sedimentation equation involving the diffusion term. Even approximate solutions of the complete Lamm equation appear to be formidably difficult for the case when the sedimentation coefficient, s, varies with pressure. The initial condition for C is assumed to be

$$C = C_0 (t = 0, r_0 < r < r_1) \qquad (2)$$

where r_0 and r_1 are, respectively, the radii of the meniscus and the bottom of the cell.

Since there is no flow of material across the menis-

(2) H. Mosimann and R. Signer, *Helv. Chim. Acta*, **27**, 1123 (1944).
(3) J. Oth and V. Desreux, *Bull. soc. chim. Belges*, **63**, 133 (1954).
(4) P. Y. Cheng and H. K. Schachman, THIS JOURNAL, **77**, 1498 (1955).
(5) S. Singer, *J. Polymer Sci.*, **2**, 290 (1947).
(6) O. Lamm, *Arkiv Mat., Astr. o. Fys.*, **21B**, No. 2 (1929).
(7) H. Fujita, *J. Chem. Phys.*, **24**, 1084 (1956).

cus and the bottom of the cell, the boundary conditions

$$D\frac{\partial C}{\partial r} - rs\omega^2 C = 0 (t > 0, r = r_0) \qquad (3)$$

$$D\frac{\partial C}{\partial r} - rs\omega^2 C = 0 (t > 0, r = r_1) \qquad (4)$$

must be satisfied, where D is the diffusion coefficient. When $D = 0$ as in the present treatment, these reduce to

$$C = 0 \ (t > 0, r = r_0) \qquad (5)$$
$$C = 0 \ (t > 0, r = r_1) \qquad (6)$$

Since equation 1 is first order with respect to r, its general solution cannot fulfill both boundary conditions 5 and 6. One of them must be abandoned.

As noted above, the sedimentation coefficient, s, should be small if the diffusion term is omitted, as in equation 1, from the complete Lamm equation. Accordingly, it may be assumed that the sign of s is maintained the same throughout the cell, although its magnitude may change from position to position owing to the pressure effect. Here it is assumed that the sign of s is positive throughout the cell, because such a case is of primary interest from the practical point of view. Then, dissolved solute molecules travel through the cell toward the bottom by ultracentrifugation and accumulate there with the passing of time. Boundary condition 6 apparently contradicts this physical picture and, therefore, must be discarded. Thus, our problem is reduced to solving equation 1 subject to initial condition 2 and boundary condition 5.

To facilitate the analysis which follows, we introduce the dimensionless variables

$$C/C_0 = \theta, \ (r/r_0)^2 = y, \ 2\omega^2 s_0^0 t = \tau, \ s/s_0^0 = \sigma$$

where s_0^0 is the value of s at $C = 0$ and a pressure of one atmosphere. Equation 1, initial condition 2 and boundary condition 5 are then written

$$\frac{\partial \theta}{\partial \tau} = -\frac{\partial}{\partial y}(y\theta\sigma) \qquad (7)$$

$$\theta = 1 (\tau = 0, 1 < y < y_1) \qquad (8)$$

$$\theta = 0 (\tau > 0, y = 1) \qquad (9)$$

where $y_1 = (r_1/r_0)^2$.

I. The Case in which s Depends on Pressure Alone

The sedimentation coefficient s is defined as the velocity of sedimentation per unit field of force and is assumed to be given by the Svedberg relation

$$s = M(1 - \rho\bar{v})/f \qquad (10)$$

where M is the molecular weight of the solute, ρ is the density of the solvent, $\bar{v}$ is the specific volume of the solute and f is the frictional coefficient of the solute molecule.

We denote the values of ρ, $\bar{v}$ and f at a pressure of one atmosphere by ρ_0, $\bar{v}_0$ and f_0, respectively. With Oth and Desreux[3] we assume that

$$\rho = \rho_0(1 + \beta p) \qquad (11)$$

$$\bar{v} = \bar{v}_0\left(1 - \frac{1}{\kappa}p\right) \qquad (12)$$

$$f = f_0(1 + \lambda p) \qquad (13)$$

where p is the pressure measured from 1 atm., β is the compressibility of the solvent, κ is the bulk modulus of the solute and λ is a certain constant.

As for β and κ there are numerous experimental data but very little is known about λ. Introduction of equations 11, 12 and 13 in equation 10 leads to

$$s = s_0[1 - \mu p + O(p^2)] \tag{14}$$

where

$$s_0 = M(1 - \rho_0 \bar{v}_0)/f_0 \tag{15}$$

and

$$\mu = \lambda + \frac{\rho_0 \bar{v}_0(\beta - 1/\kappa)}{1 - \rho_0 \bar{v}_0} \tag{16}$$

It is apparent that equation 14 ceases to be valid for systems in which $\rho_0 \bar{v}_0$ is close to unity. However, since in such systems the magnitude of s becomes very small (see equation 15), the basic equation 7 of the present analysis also ceases to be valid, as has been noted in the foregoing lines. Hence, we proceed with our analysis assuming equation 14 to be valid.

As a first approximation, we neglect terms in equation 14 higher than $O(p)$. Thus

$$s = s_0(1 - \mu p) \tag{17}$$

This procedure was also adopted by Oth and Desreux[3] in their study and is considered to be satisfactory for most practical purposes.

The pressure distribution in the cell can be determined by

$$\frac{dp r}{dr} = \rho \omega^2 r^2 \tag{18}$$

Introduction of equation 11, and determination of the integration constant with $p = 0$ at $r = r_0$ yields

$$p = \frac{1}{\beta} \left\{ \frac{e^{\nu y}}{\sqrt{y}} \left[e^{-\nu} + \frac{\sqrt{\pi}}{2\sqrt{\nu}} (\Phi(\sqrt{\nu}y) - \Phi(\sqrt{\nu})) \right] - 1 \right\} \tag{19}$$

where $\nu = \frac{1}{2}\beta\rho_0\omega^2 r_0^2$ and Φ is the error function. As a numerical example, we take

$$\omega^2 = 40 \times 10^6 \text{ rad.}^2 \text{ sec.}^{-2}$$
$$r_0 = 6 \text{ cm.}$$
$$\rho_0 = 0.792 \text{ g. cm.}^{-3}$$
$$\beta = 82 \times 10^{-6} \text{ atm.}^{-1}$$

In Fig. 1 we show the p vs. y curve for this case as computed from equation 19. Assuming that the distance from the meniscus to the bottom of the cell is 1.0 cm., $y = 1.3611$ corresponds to the cell bottom, where p is seen to amount to about 200 atm. Since for many liquids equation 19 may be approximated, within the range of y obtaining in ordinary sedimentation cells, by

$$p = (1/2)\omega^2 r_0^2 \rho_0(y - 1) \tag{20}$$

equation 17 becomes

$$s = s_0[1 - m(y - 1)] \tag{21}$$

where m stands for

$$m = (1/2)\mu\omega^2 r_0^2 \rho_0 \tag{22}$$

Thus, in this approximation, s is a linear function of y. It must be remembered that in order that equation 21 may hold, the product, $m(y - 1)$, should be sufficiently small in comparison with unity. This condition is likely to hold for most systems, except for the ones in which $\rho_0 \bar{v}_0$ is close to unity.

In this section, we consider the case in which s

depends only on pressure. Then, s_0 in equation 21 may be taken as s_0^0 defined previously, and we have

$$\sigma = 1 - m(y - 1) \tag{23}$$

Introduction of equation 23 in equation 7 gives

$$\frac{\partial\theta}{\partial\tau} = -\frac{\partial}{\partial y} \{\theta y[1 - m(y - 1)]\} \tag{24}$$

The characteristic equation for this partial differential equation of the first order is

$$\frac{d\tau}{1} = \frac{dy}{y[1 - m(y - 1)]} = -\frac{d\theta}{\theta(1 - 2my)} \tag{25}$$

from which we have readily

$$\tau - \frac{1}{1 + m} \ln \frac{y}{1 - m(y - 1)} = a \tag{26}$$

$$\theta y[1 - m(y - 1)] = b \tag{27}$$

where a and b are integration constants. The general solution of equation 24 thus reads

$$\theta = \frac{F\left[\tau - \dfrac{1}{1 + m} \ln \dfrac{y}{1 - m(y - 1)}\right]}{y[1 - m(y - 1)]} \tag{28}$$

where F stands for an arbitrary function of its argument.

Introduction of initial condition 8 into equation 28 leads to

$$1 = \frac{F\left[-\dfrac{1}{1 + m} \ln \dfrac{y}{1 - m(y - 1)}\right]}{y[1 - m(y - 1)]} \quad (1 < y < y_1) \tag{29}$$

which permits determination of the functional form of $F(z)$ in the range of z from $-z_1$ to zero. Thus

$$F(z) = \frac{(1 + m)^2 e^{-(1 + m)z}}{[1 + me^{-(1 + m)z}]^2} \quad (-z_1 < z < 0) \tag{30}$$

where

$$z_1 = \frac{1}{1 + m} \ln \frac{y_1}{1 - m(y_1 - 1)} \tag{31}$$

Introduction of boundary condition 9 into equation 28 determines the form of $F(z)$ for $z > 0$. Thus

$$F(z) = 0 \quad (z > 0) \tag{32}$$

Hence, the desired solution of equation 24 subject to the conditions 8 and 9 is given by

$$\theta = 0 \quad \left(\tau > \frac{1}{1 + m} \ln \frac{y}{1 - m(y - 1)}\right)$$

$$\theta = \frac{(1 + m)^2 e^{-(1 + m)\tau}}{[1 + m - my(1 - e^{-(1 + m)\tau})]^2}$$

$$\left(\tau < \frac{1}{1 + m} \ln \frac{y}{1 - m(y - 1)}\right) \tag{33}$$

Denoting by y_* the value of y determined by

$$\tau = \frac{1}{1 + m} \ln \frac{y}{1 - m(y - 1)} \tag{34}$$

we have

$$y_* = \frac{1 + m}{m + e^{-(1 + m)\tau}} \tag{35}$$

and it is found from equation 33 that

$$\lim_{y \to y_* - 0} \theta = 0 \tag{36}$$

$$\lim_{y \to y_* + 0} \theta = \frac{1}{(1 + m)^2} [e^{-(1 + m)\tau} + 2m + m^2 e^{(1 + m)\tau}] \tag{37}$$

Consequently, the θ vs. y relation (concentration-distance curve) is represented by a discontinuous
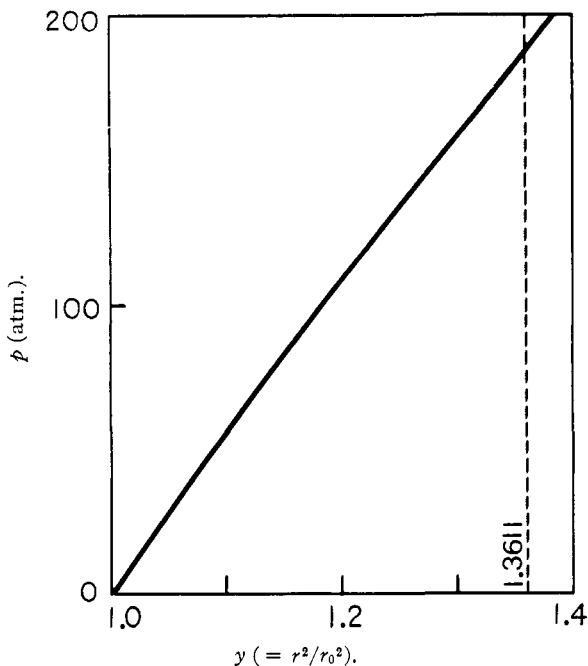
Fig. 1.—Pressure distribution in the cell.

Fig. 2.—Schematic representation of the concentration-distance curve when s depends on pressure.

curve with the break at $y = y_*$, as shown schematically in Fig. 2. It should be noted that the portion of the curve for y larger than y_* is no longer horizontal but shows (when $m > 0$) an increasing upward curvature. It is also important to note that the "square dilution law," which should result in $(\theta \, y_*) = 1$, no longer holds when s depends on pressure.

Next, we derive the equation for the concentration gradient, $\partial C/\partial r$. Since

$$\frac{\partial C}{\partial r} = \frac{C_0}{r_0}\frac{\partial \theta}{\partial \sqrt{y}} = \frac{2C_0}{r_0}\left(\frac{r}{r_0}\right)\frac{\partial \theta}{\partial y}$$

it is found, by substituting equation 33 in this equation, that

$$\frac{\partial C}{\partial r} = 0 \quad (r_0 < r < r_*) \tag{38}$$

$$\frac{\partial C}{\partial r} = \infty \quad (r = r_{*-0}) \tag{39}$$

$$\frac{\partial C}{\partial r} = \frac{4C_0 m}{r_0(1 + m)^{7/2}} e^{2(1+m)\tau}[1 - e^{-(1+m)\tau}][m + e^{-(1+m)\tau}]^{5/2}$$

$$(r = r_{*+0}) \tag{40}$$

$$\frac{\partial C}{\partial r} =$$

$$\frac{4mC_0(1 + m)^2}{r_0}\frac{r}{r_0}\frac{e^{-(1+m)\tau}[1 - e^{-(1+m)\tau}]}{\left\{1 + m - m\left(\dfrac{r}{r_0}\right)^2[1 - e^{-(1+m)\tau}]\right\}^3}$$

$$(r_* < r < r_1) \tag{41}$$

where r_* is the value of r corresponding to y_*. For small enough values of m and τ equation 41 may be written approximately

$$\frac{\partial C}{\partial r} = \frac{4mC_0}{r_0}\left(\frac{r}{r_0}\right)e^{-(1+m)\tau} \tag{42}$$

$$\times \frac{[1 - e^{-(1+m)\tau}]}{1 + m}\left\{1 + \frac{3m}{1 + m}\left(\frac{r}{r_0}\right)^2[1 - e^{-(1+m)\tau}]\right\}$$

A numerical example of the concentration gradient curve computed from equations 38–41 is shown in Fig. 3. As observed from this figure, when s de-
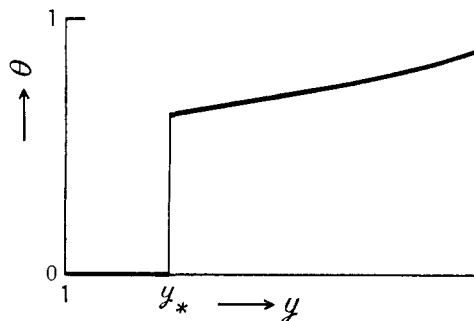
pends on pressure, the concentration gradient curve does not return to the base line after passing the maximum. In practical systems where the effect of diffusion is operating, a shallow minimum having a finite height will appear in the region of the concentration gradient curves beyond their maximum.

It follows from equation 35 that

$$\ln y_* = (1 + m)\tau + \ln(1 + m)/[1 + me^{(1+m)\tau}] \tag{43}$$

Hence, when s depends on pressure, plots of $\ln y_*$ are no longer linear against time, However, it can be shown from equation 43 that

$$d(\ln y_*)/2d(\omega^2 t) = s_0[1 - m(y_* - 1)] \tag{44}$$

so that plots of $d(\ln y_*)/2d(\omega^2 t)$ against $(y_* - 1)$ are linear. By extrapolating back the resulting straight line to $y_* - 1 = 0$, the value of s_0 is determined, while from the slope the value of m is obtained. From data obtained at different rotations, values of $d(\ln y_*)/2d(\omega^2 t)$ at a fixed value of y_* may be plotted against ω^2. Because m is proportional to ω^2, this plot should be linear according to equation 44. The value of s_0 may be obtained from the intercept of the straight line at $\omega^2 = 0$.
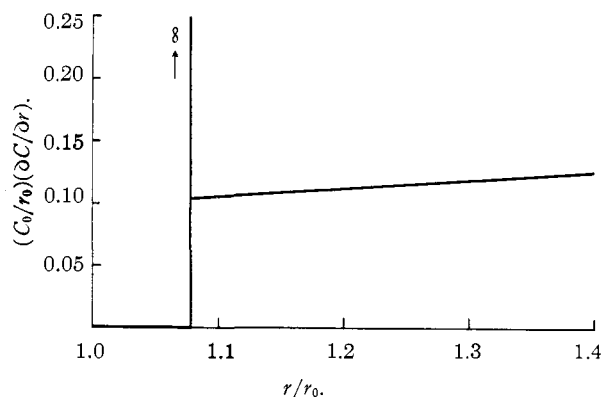

Fig. 3.—A numerical illustration of the concentration gradient-distance curve when s depends on pressure.

It must be pointed out that these two methods for evaluating s_0 are not new but have already been described by Oth and Desreux,[3] who derived them on the basis of a less rigorous treatment than that described here. As to experimental tests of these methods, reference is made to Oth and Desreux's paper.

It is rather difficult to obtain values of $d(\ln y_*)/2d(\omega^2 t)$ with high precision from experimental $\ln y_*$

vs. $2\omega^2 t$ curves, so that use of equation 44 may not always be practical. The slope of the straight line connecting any point on a given experimental $\ln y_*$ *vs.* $2\omega^2 t$ curve with the origin is evaluated more accurately and easily than the tangent $d(\ln y_*)/2d(\omega^2 t)$. The equation for this slope, derived from equation 35, is

$$\frac{\ln y_*}{2\omega^2 t} = s_0 \left[1 - \frac{m}{2}(y_* - 1) + \frac{m(m-1)}{12}(y_* - 1)^2 + \cdots \right] \quad (45)$$

Within the degree of the approximations adopted in this paper, this equation may be approximated satisfactorily by

$$\frac{\ln y_*}{2\omega^2 t} = s_0 \left[1 - \frac{m}{2}(y_* - 1) \right] \quad (46)$$

Except for the numerical factor multiplying m, this has the same form as equation 44 and, therefore, can be used for evaluating s_0 according to the same procedures as described above for equation 44. Since, as mentioned above, the quantity on the left side of this equation is evaluated accurately and easily, more reliable values of s_0 should be obtained from equation 46 than from equation 44.

II. The Case in which s Depends Both on Pressure and Concentration

Before treating the case in which s depends both on pressure and concentration, we consider the case in which s depends on concentration only according to the relation

$$s = \frac{s_0}{1 + kC} \quad (47)$$

in order to understand a certain characteristic feature of solutions for which the basic equation 47 may be taken as s_0^0 defined previously. Then equation 7 takes the form

$$\frac{\partial \theta}{\partial \tau} = - \frac{\partial}{\partial y}\left(\frac{y\theta}{1 + \alpha\theta} \right) \quad (48)$$

where α is

$$\alpha = kC_0 \quad (49)$$

and is assumed to be positive.

Solution of equation 48 by means of the method of characteristics gives the general solution in the form

$$\tau + \alpha\theta + \ln \theta = F\left(\frac{y\theta}{1 + \alpha\theta} \right) \quad (50)$$

where F is an arbitrary function of its argument. Introduction of initial condition 8 in equation 50 determines the form of $F(z)$ for z from $1/(1 + \alpha)$ to $y_1/(1 + \alpha)$. Thus

$$F(z) = \alpha \left(\frac{1}{1+\alpha} < z < \frac{y_1}{1+\alpha} \right) \quad (51)$$

Substitution of boundary condition 9 in equation 50 yields

$$F(0) = - \infty \quad (52)$$

From equations 50 and 51 we have

$$\tau = \alpha(1 - \theta) - \ln \theta \ (\tau > 0, \Theta(\tau) < y < y_1 \Theta(\tau)) \quad (53)$$

where $\Theta(\tau)$ is such a function of τ that can be determined from a set of equations

$$\Theta(\tau) = (1 + \alpha\theta)/\theta(1 + \alpha) \quad (54)$$

$$\tau = \alpha(1 - \theta) - \ln \theta \quad (55)$$

On the other hand, it follows from equations 50 and 52 that

$$\theta = 0(\tau > 0, y \geqq 1) \quad (56)$$

From equations 53 and 56 it is found that for $\tau > 0$, θ as a function of y is two-valued in the range of y such that

$$y_1 \Theta(\tau) > y > \Theta(\tau) \quad (57)$$

and is one-valued in the remaining range of y, *i.e.*,[8]

$$\Theta(\tau) > y \geqq 1 \quad (58)$$

This rather peculiar behavior of the solution of equation 48 is attributed to the non-linearity of the basic sedimentation equation, which makes its appearance when s depends on concentration C.

Physically, the concentration must be a one-valued function of time and position; it must be made up from solutions 53 and 56 so that they may satisfy this physical requirement. For this purpose we make up a one-valued function such that

$$\theta = 0 \ (\tau > 0, y_*(\tau) > y \geqq 1)$$
$$\theta = \exp[-\tau + \alpha(1 - \theta)] \ (\tau > 0, y_1 > y > y_*(\tau)) \quad (59)$$

where $y_*(\tau)$ is an arbitrary function of τ which satisfies an inequality

$$y_1 \Theta(\tau) > y_*(\tau) > \Theta(\tau) \quad (60)$$

and the limiting property

$$\lim_{\tau \to 0} y_*(\tau) = 1 \quad (61)$$

It is readily confirmed that the function so made up is one-valued for time and position and satisfies the basic equation 49, initial condition 8 and boundary condition 9. It is represented by a step function having a discontinuous point at $y = y_*(\tau)$, as shown in Fig. 4. The form of $y_*(\tau)$ as a function of τ can be determined from the basic equation 48 by integrating it with respect to y from $y - \delta$ to $y + \delta$ and letting δ approach zero. This process leads to the differential equation for $y_*(\tau)$ of the form

$$\frac{dy_*}{d\tau} = \frac{y_*}{1 + \alpha\theta_*} \quad (62)$$

where θ_* is

$$\theta_* = \exp[- \tau + \alpha(1 - \theta_*)] \quad (63)$$

Equation 62 can be integrated to give

$$y_* = 1/\theta_* \quad (64)$$

where equation 61 has been used to determine the constant of integration. Substitution of θ_* from equation 64 in equation 63 yields

$$\tau = [\alpha(1/y_*) - 1] + \ln y_* \quad (65)$$

which gives y_* as a function of τ but cannot be solved explicitly for y_*. It can be shown easily that $y_*(\tau)$ determined in this way satisfies the condition 60. Thus, the desired solution of the problem is given by equation 59 with $y_*(\tau)$ determined from equation 65. It is found that this solution agrees with that obtained by previous investigators who used a more or less intuitional method (see, for example, Alberty[9]). It may be noted that equation

(8) It can be shown from equations 54 and 55 that for $\tau > 0$ and $\alpha > 0 \ \Theta(\tau)$ is larger than unity.

(9) R. A. Alberty, THIS JOURNAL, **76**, 3733 (1954).

64 shows that the square dilution law holds, as should be in this case.

Now we proceed to consider a more general case where s depends not only on C, according to equation 48, but also on pressure according to equation 21. In this case, we may write

$$s = \frac{s_0^0}{1 + kC} [1 - m(y - 1)] \qquad (66)$$

Accordingly, equation 7 takes the form

$$\frac{\partial \theta}{\partial \tau} = - \frac{\partial}{\partial y} \left\{ \left(\frac{y\theta}{1 + \alpha\theta} \right) [1 - m(y - 1)] \right\} \qquad (67)$$

Application of the method of characteristics yield the general solution of equation 67 in the form

$$\tau - \frac{1}{[4ma\alpha - (1 + m)^2]} \left\{ \frac{a\alpha(2my - 1 - m)}{my^2 - (1 + m)y + a\alpha} + \frac{2[2ma\alpha - (1 + m)^2]}{[(1 + m)^2 - 4ma\alpha]^{1/2}} \right.$$

$$\left. \times \tanh^{-1} \frac{2my - 1 - m}{[(1 + m)^2 - 4ma\alpha]^{1/2}} \right\} = F(a) \qquad (68)$$

where F is again an arbitrary function of its argument, and a stands for

$$a = y(1 + m - my)\theta/(1 + \alpha\theta) \qquad (69)$$

The procedure for determining the functional form of F in terms of the initial and boundary conditions is entirely the same as illustrated above, with s dependent on C only; after making up a one-valued function from the two-valued solution then obtained—owing to the non-linearity of the basic equation 67—we obtain the final solution in the form.[10]

$$\theta = 0(\tau > 0, y^*(\tau) > y \geqq 1) \qquad (70)$$

$$\tau = \frac{1}{[4ma\alpha - (1 + m)^2]} \left\{ \frac{a\alpha(2my - 1 - m)}{my^2 - (1 + m)y + a\alpha} - \alpha[(1 + m)^2 - 4ma(1 + \alpha)]^{1/2} + \frac{2[2ma\alpha - (1 + m)^2]}{[(1 + m)^2 - 4ma\alpha]^{1/2}} \left[\tanh^{-1} \frac{2my - 1 - m}{[(1 + m)^2 - 4ma\alpha]^{1/2}} + \tanh^{-1} \left[\frac{(1 + m)^2 - 4(1 + \alpha)ma}{(1 + m)^2 - 4ma\alpha} \right]^{1/2} \right] \right\}$$

$$(\tau > 0, y_1 > y > y_*(\tau)) \qquad (71)$$

Using the same procedure as before, it is shown that $y_*(\tau)$ is determined from

$$\frac{dy_*}{d\tau} = \frac{y_*}{1 + \alpha\theta_*} [1 - m(y_* - 1)] \qquad (72)$$

where θ_* represents the value of θ to be determined from equation 71 at $y = y_*$. Equations 70 and 71 indicate that the concentration curve for this case is again a step function having a discontinuous point at $y = y_*$, but the portion of it beyond y_* is no longer horizontal. To evaluate this curve numerically, the position of the discontinuous point, y_*, must first be determined as a function of τ. However, the analytical integration of equation 72 is apparently impossible, and even its numerical solutions appear to be exceedingly involved. Thus, in this paper we shall not try to obtain numerical information about the solution.

It can be confirmed by carrying out simple limiting calculations that equation 71 reduces, in the limit $m \to 0$, to

$$\tau = \alpha(1 - \theta) - \ln \theta \qquad (73)$$
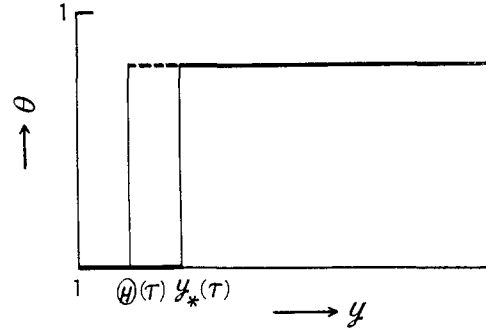
Fig. 4.—Schematic representation of the concentration-distance curve when s depends only on concentration.

while, in the limit $\alpha \to 0$, to

$$\theta = \frac{(1 + m)^2 e^{-(1 + m)\tau}}{\{1 + m - my[1 - e^{-(1 + m)\tau}]\}^2} \qquad (74)$$

These equations agree with the results obtained previously as they should. It is also shown that equation 72 yields, in these limits, the corresponding previous results.

Finally, approximate equations which are useful for sufficiently small m are derived from equations 71 and 72. After some involved calculations, equation 71 is expanded in powers of m in the form

$$\tau = \alpha(1 - \theta) - \ln \theta + m \left\{ \left(1 - \frac{4y\theta\alpha}{1 + \alpha\theta} \right) \ln \theta + (1 - \theta) \left[2 \left(\frac{1 + \alpha^2\theta}{1 + \alpha\theta} \right) y - \alpha \right] \right\} + O(m^2) \qquad (75)$$

Neglecting higher terms, there results

$$y = \frac{(1 + \alpha\theta)\{\tau - [\alpha(1 - \theta) - \ln \theta](1 - m)\}}{m[2(1 - \theta)(1 + \alpha^2\theta) - 4\alpha\theta\ln \theta]} \qquad (76)$$

After putting $y = y_*$, we differentiate this with respect to τ and insert the resulting equation in equation 72. We then have

$$\frac{d\theta_*}{dy_*} = - \frac{\theta_*}{y_*} f(\theta_*, y_*) \qquad (77)$$

with

$$f(\theta_*, y_*) = 1 - \frac{my_*}{(1 + \alpha\theta_*)^3} [1 + 5\alpha\theta_* + (2\alpha^3 + 3\alpha^2 - 2\alpha)\theta_*^2 - \alpha^3\theta_*^3 - 4\alpha^2\theta_*^2 \ln \theta_*] \qquad (78)$$

where terms higher than $O(m)$ have been ignored. Equations 78 cannot yet be integrated analytically but may be solved either numerically or graphically without difficulty. Substitution of solutions obtained into equation 76 (in which y and θ must be taken as y_* and θ_*, respectively) provides the relation between y_* and τ. The concentration curve for $y = y_*$ is then computed from equation 76.

It should be noted that in this case the square dilution law no longer holds (when $m = 0$, equation 77 is integrated to give $\theta_* y_* = 1$, which yields the square dilution law), so that we cannot write equation 72 in the form

$$\frac{dy_*}{d\tau_*} = \frac{1}{1 + \alpha(1/y_*)} [1 - m(y_* - 1)] \qquad (79)$$

as Oth and Desreux[3] have adopted in their paper. However, when m is sufficiently small, equation 79

may be employed as a useful approximate equation. As for an application of equation 79, reference is made to Oth and Desreux's paper.

J. W. Williams, R. L. Baldwin and L. J. Gosting in this work. The work was made possible by a grant-in-aid from the Public Health Service, National Institutes of Health.

MADISON 6, WISCONSIN

Characterization of the Monomer and Dimer of Tobacco Mosaic Virus by Transient Electric Birefringence[1]

BY CHESTER T. O'KONSKI AND ARTHUR J. HALTNER[2]

The rotational diffusion constant of the monomer unit of tobacco mosaic virus in dilute aqueous solution was found to be 333 sec.$^{-1}$ from transient electric birefringence measurements of a number of preparations. This value corresponds to a length of 3416 ± 50 Å., which is significantly greater than 2980 ± 10 Å., reported in the most recent electron microscope study. Assuming a compact circular rod, 3416 Å. long, and employing the X-ray diameter and the measured specific volume, the molecular weight is 50×10^6, in agreement with the result of an independent precise method. The new value for the length is discussed with reference to data from other types of measurements. Evidence was obtained for the existence of an end-to-end dimer in all but one of the preparations. Because the constant for rotational diffusion of an elongated macromolecule about its short axis depends most critically upon the length, transient electric birefringence is an especially sensitive method for measuring the lengths of rigid macromolecules. Improved experimental methods are described.

Introduction

As the physical characteristics of the tobacco mosaic virus (TMV) have been studied intensively by many different methods, it is an excellent material for model studies of the phenomenon of electric birefringence. According to prevailing ideas[3]–[8] on the subject, the pure crystalline virus probably consists of uniform rod-shaped macromolecules which become dispersed as independent units in dilute aqueous solutions. For quantitative measurements of the magnitude of the electric birefringence in such solutions, it is necessary to determine if a given preparation contains a single well-defined species, and to find the conditions under which a solution will behave ideally, that is, to ascertain the dilution required for the macromolecules to respond as individual kinetic units to the stress produced by an applied electric field.

In the course of investigations of the orienting mechanisms in electric birefringence, several TMV preparations were studied by the transient technique. In four of the more homogeneous preparations, there was found predominantly a species with a rotational diffusion constant of 333 sec.$^{-1}$, corresponding to the monomeric rods. In three of the four preparations there was another species of rotational diffusion constant around 56 sec.$^{-1}$, which suggests an end-to-end rigid dimer. Because the rotational diffusion constant is a sensitive function of the length of a rod-shaped macromolecule, relatively precise values of length can be calculated. The monomer length, 3416 Å., is significantly greater than the recent value of Williams and Steere[9] obtained by electron microscopy. When a molecular weight is computed from our value of the length the X-ray diameter of the rod and the partial specific volume, assuming a circular compact cross-section, one obtains 50×10^6, in agreement with the value of Williams, Backus and Steere,[10] obtained by a direct weighing and particle counting technique. Accordingly, the concept of a hexagonal cross-section, introduced[10] to produce consistency between certain length, density, molecular weight and lattice spacing measurements on the crystalline virus, is not supported by this research.

The occurrence of end-to-end dimers may have biological implications, and is of interest in the characterization of the macromolecules by other techniques, such as flow birefringence and light scattering, which do not easily permit clear resolution of the components. For these reasons, a detailed account of the results on these four preparations is presented here. Investigations concerning the nature of the orienting mechanism in electric fields, and the effects of mutual interactions between the macromolecules observed in somewhat more concentrated solutions, will be reported later.

The Transient Electric Birefringence Phenomenon.—When a fluid is subjected to electric stress, polar or electrically anisotropic molecules interact with the local electric field and the general result is that the molecular orientations are no longer random. Then, if the molecules are optically anisotropic, the fluid becomes doubly refracting.[11]

(1) Presented before the Section on Chemistry at the 121st meeting of the American Association for the Advancement of Science, Berkeley, California, Dec. 26, 1954. This paper is based upon the thesis submitted by Arthur J. Haltner in January, 1955, in partial fulfillment of the requirements for the Ph.D. in Chemistry.

(2) National Science Foundation Predoctoral Fellow, 1953–1954.

(3) W. M. Stanley, *Handbuch Virusforschung*, **1**, 477 (1938).

(4) M. A. Lauffer, *J. Biol. Chem.*, **151**, 627 (1943).

(5) G. O. Oster and W. M. Stanley, *Brit. J. Exp. Path.*, **27**, 261 (1946).

(6) T. Sigurgeirsson and W. M. Stanley, *Phytopathology*, **37**, 26 (1947).

(7) W. N. Takahashi and T. E. Rawlins, *ibid.*, **39**, 672 (1949).

(8) H. K. Schachman, THIS JOURNAL, **73**, 4808 (1951).

(9) R. C. Williams and R. L. Steere, *ibid.*, **73**, 2057 (1951).

(10) R. C. Williams, R. C. Backus and R. L. Steere, *ibid.*, **73**, 2062 (1951).

(11) M. Born, "Optik," J. Springer, Berlin, 1933; Edwards Bros., Ann Arbor, Mich., 1943.